13

Studies of Cardio Toxin Protein Adsorption on Mixed Self-Assembled Monolayers Using Molecular Dynamics Simulations

Shih-Wei Hung[1], Pai-Yi Hsiao[1] and Ching-Chang Chieng[2]
[1]*Department of Engineering and System Science*
National Tsing Hua University, Hsinchu
[2]*Department of Mechanical and Biomedical Engineering*
City University of Hong Kong, Kowloon
[1]*Taiwan*
[2]*Hong Kong*

1. Introduction

To understand protein adsorption on a surface is very important in bio-related domains of technology and application such as biomaterials, implant biocompatibility, and biosensor technology. (Gray 2004) Self-assembled monolayers (SAMs) are excellent model surfaces for biology and biochemistry because they are stable, highly ordered, easy to prepare, and provide a wide range of organic functionality. (Love et al. 2005) Previous experimental studies (Ostuni et al. 2003; Prime & G.M. Whitesides 1991) have indicated that hydrophobic interactions are the major mechanism for protein adsorption on surfaces, and the dehydration of both the protein and hydrophobic SAMs provides an entropic driving force for protein adsorption. (Ostuni et al. 2003) Nonetheless, there are still many questions needed to be clarified and difficult to be investigated in experiments. Molecular dynamics (MD) simulation is a powerful tool that is able to investigate the atomic details of a molecular system. This paper summarizes the investigations of proteins adsorption on alkanethiol SAMs by means of MD simulations in order to expand the limited information that the experiments can provide. (Hung et al.2006; Hung et al.2010; Hung et al. 2011)

MD simulation has been applied to study the mechanisms of proteins adsorption on various SAMs and has provided valuable information. For example, Tobias *et al.* (Tobias et al. 1996) studied cytochrome-c (Cyt-c) covalently tethered to hydrophobic (methyl-terminated) and hydrophilic (thiol-terminated) SAMs. In their model, water molecules were not modeled explicitly. They found that Cyt-c was completely excluded from the hydrophobic SAM surface but partially dissolved on the hydrophilic SAM surface. In a follow-up study, Nordgren *et al.* (Nordgren et al. 2002) reported that the larger perturbation of Cyt-c structure occurred on hydrophilic SAM surfaces rather than on

hydrophobic SAM surfaces using explicit water molecule model. They found that the protein molecule was surrounded by the water molecules, resulting in the reduction of the interaction between the protein and the surface. Zhou *et al.* (Zhou et al. 2004) investigated the orientation and conformation of Cyt-c on carboxyl-terminated SAM using a combined method of Monte Carlo (MC) and MD simulations. Their results showed that the preferable orientation of an adsorbed protein can be obtained by a strongly charged surface but the protein may lose its bioactivity due to the large conformational change. To understand surface resistance to protein adsorption, Jiang and his coworkers(Hower et al. 2006; Zheng et al. 2004; Zheng et al. 2005) studied lysozyme adsorption on various SAM surfaces with terminal methyl, hydroxyl, oligo (ethylene glycol) (OEG), mannitol, and sorbitol groups by a hybrid MC and MD simulation. They concluded that the resistance of protein adsorption to a surface was due to the tightly bound, structured water layer directly above the surface. Agashe *et al.* (Agashe et al. 2005) utilized MD simulations to investigate the adsorption of the γ-chain fragment of fibrinogen on SAM surfaces with five different terminal groups: methyl, hydroxyl, carboxyl, amino and OEG. The fibrinogen fragment did not show conformational rearrangements; rather it underwent rotational and translational motions until low-energy orientations were achieved. The above studies demonstrated that MD simulation is a useful and important tool to study protein adsorption on various SAM surfaces.

Not only the static properties, such as orientation and potential energy, but also the dynamic information about the process of CTX binding to the membrane are of interest. The dynamic biological process and the corresponding information, such as the structural change, adsorption force, interaction energy, and potential of mean force (PMF), can be investigated by steered molecular dynamics (SMD) simulation. (Israelewitz et al. 2001) The PMF is the equilibrium free energy difference along the reaction coordinate, which is an important thermodynamic quantity characterizing the dynamic process. (Kirkwood 1935) Calculation methods for PMF had been reviewed and classified as either equilibrium or non-equilibrium approaches.(Ytreberg, Swendsen, and Zuckerman 2006) The equilibrium approaches, for example, the umbrella sampling method, (Torrie & Valleau 1977) need large computer resources because they rely on fully sampled equilibrium simulations performed at each stage of the PMF calculation. The non-equilibrium approaches, for example, using Jarzynski's remarkable equality (Jarzynski 1997) from SMD simulations, has the potential to provide very rapid estimates of PMF. However, the use of Jarzynski's equality suffers from significant bias and error when the pulling velocity is too high or the number of trajectories sampled is insufficient.(Gore, Ritort, and Bustamante 2003)

CTX is a cytotoxic β-sheet basic polypeptide which is known to cause membrane leakage in many cells including human erythrocytes and phospholipid membrane vesicles.(Dufton and Hider 1988) The three-dimensional structures of various CTX homologues in both aqueous and micellar environments are available.(S C Sue et al. 2001; Dauplais et al. 1995) The interactions between CTX and lipid membranes have been widely studied by various methods, such as Fourier transform infrared spectroscopy, (Huang et al. 2003; Forouhar et al. 2003) nuclear magnetic resonance (NMR) spectroscopy, (Dubovskii et al. 2005) and computer simulation.(Levtsova et al. 2009; R G Efremov et al. 2004) CTXs do not easily adopt large conformational changes due to the existence of four

disulfide bonds in their chemical structure. Therefore, they are good candidates in experimental study of protein adsorption on SAM surfaces. MD simulations can help, furthermore, in the understanding of the interaction of CTX-SAM system.

In our earlier study, (Hung et al. 2006) the binding energy of protein molecules to SAM surfaces of different mixing composition of alkanethiols chains was investigated. We found that the binding energy was enhanced due to the increasing of the hydrophobic area on the SAM surface. In that study, we focused on the enthalpic contribution of the hydrophobic interaction between a CTX molecule and SAM surfaces, and thus a solvent model of distance-dependent dielectric function was used (Ramstein & Lavery 1988) instead of explicit water molecules. However, the hydrophobic interaction is primarily driven by entropy (Chandler 2005) and it has been shown by many groups (Hower et al. 2006; Zheng et al. 2004; Zheng et al. 2005; Ostuni et al. 2003) that the water molecules on the protein-SAM interface play an important role on protein adsorption mechanism. In order to take into account both enthalpic and entropic components of hydrophobic interaction, an explicit solvent model is conducted to investigate and identify the complete physical mechanism.

Summmarizing our previous studies, MD simulations were performed to study the physical mechanism of CTX proteins adsorption on alkanethiol SAMs with different chain lengths. The dynamic information, such as structural changes and adsorption forces of CTX protein desorption from the SAM surface were investigated by means of SMD simulations. The dependence of the dynamic information on the pulling velocity was illustrated. The PMFs were calculated by the umbrella sampling method for better interpretation of the desorption process.

2. Model system and methodology

2.1 Simulation model

In order to study the adsorption of a CTX protein on the surfaces composing of mixed *alkanethiol SAM* growing on Au (111) substrate, two types of alkanethiol chains, $S(CH_2)_5CH_3$ and $S(CH_2)_9CH_3$, were composed and were denoted briefly by C5 and C9, respectively. The structure of the SAM is a $(\sqrt{3}\times\sqrt{3})R30°$ lattice on *x*-*y* plane with lattice constant equal to 0.499 nm. Each lattice point is occupied by an alkanethiol chain of either C5 or C9. Five mixing ratios were studied: χ_{C9} = 0, 0.25, 0.5, 0.75 and 1, where χ_{C9} is defined as $N_{C9}/(N_{C5}+N_{C9})$ with N_{C5} and N_{C9} representing respectively the numbers of C5 and C9 chains in the SAMs. In our studies, there were 12 chains on each side of the simulation box. Periodic boundary condition was applied in *x* and *y* directions to simulate infinitely large surface of SAMs. The Au (111) substrate was modeled by a single layer of gold atoms.

The CTX protein was modeled by the nuclear magnetic resonance (NMR) structure of CTX A3 (PDB 1I02), (Sue et al. 2001) comprised of 60 amino acid residues. The interactions between CTX and lipid membrane had been well studied by Wu's group, (Huang et al. 2003; Forouhar et al. 2003) and they found that the characteristics topology of three hydrophobic fingers (Fig. 1) played a key role in binding to lipid membranes. Hence, the CTX protein was chosen as the model system to study the protein-SAM interaction, to identify the mechanism of protein adsorbing on a SAM surface, and to understand the role of the protein hydrophobicity on the adsorption in our studies.

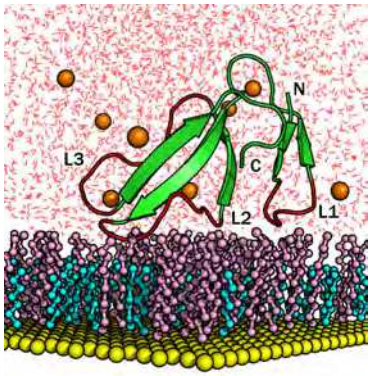

Fig. 1. Illustration of CTX adsorbed on SAM/Au (111) surface where $\chi_{C9} = 0.5$ (C5 is plotted in cyan color, C9 in pink color and gold atoms in yellow color). Water molecules are plotted in red color and the counter ions are in orange spheres. C and N indicate the C-terminus and N-terminus of the CTX protein, respectively. The three major loops, denoted by L1, L2 and L3, of CTX are colored in red. (Hung et al.2010)

2.2 Potential energy function

The potential energy function used in MD simulation included several terms describing both internal (bonded) and external (nonbonded) interactions, which ultimately determined both structure and dynamics of a molecular system. The atomic interactions inside a CTX molecule were described by the GROMOS-96(43a2) force field. (Schuler and Wilfred Van Gunsteren 2000) This force field consisted of bonded interactions, including bond, angle, dihedral and improper dihedral angle terms, and non-bonded interactions, including van der Waals (vdW) and Coulomb interactions. The complete form of this force field read

$$U = \sum_{\text{bonds}} \frac{1}{2} k_b (r - r_0)^2 + \sum_{\text{angles}} \frac{1}{2} k_\theta (\theta - \theta_0)^2 + \sum_{\text{dihedrals}} k_\varphi \left[1 + \cos\left(n\varphi - \varphi_0\right)\right] + \sum_{\text{impropers}} k_\xi (\xi - \xi_0)^2 + \sum_{\text{vdW}} 4\varepsilon_{ij} \left[\left(\frac{\sigma_{ij}}{r_{ij}} \right)^{12} - \left(\frac{\sigma_{ij}}{r_{ij}} \right)^{6} \right] + \sum_{\text{Coulombic}} \frac{q_i q_j}{4\pi\varepsilon_0 r_{ij}} \tag{1}$$

Here k_b, k_θ, k_φ, and k_ξ are the bond, angle, dihedral, and improper dihedral force constants, respectively, for the bonded interactions and r_0, θ_0, φ_0, and ξ_0 are the equilibrium values of bond length, bond angle, dihedral angle and improper dihedral angle, respectively. For the non-bonded interactions, ε is the Lennard-Jones well depth, σ is the distance at which the vdW interaction is zero, q is the charge, and r_{ij} is the distance between atoms i and j. The parameters of the vdW interaction for the cross interactions between atoms i and j were obtained by the geometry combination rule. The alkanethiol chains in SAMs were modeled by the united-atom model of Hautman and Klein model (Hautman & Klein 1989), given as

$$U = \sum_{\text{angles}} \frac{1}{2} k_\theta (\theta - \theta_0)^2 + \sum_{\text{dihedrals}} \sum_{n=0}^{5} C_n \left[\cos\left(\varphi - 180^\circ\right)\right]^n + \sum_{\text{vdW}} 4\varepsilon_{ij} \left[\left(\frac{\sigma_{ij}}{r_{ij}} \right)^{12} - \left(\frac{\sigma_{ij}}{r_{ij}} \right)^{6} \right] \tag{2}$$

In this model, the dihedral potential took the form of Ryckaert-Bellemans, (Ryckaert & Bellemans 1978) in which the potential was expanded in a series of cosine function of the dihedral angle φ with C_n = 9.28, 12.16, -13.12, -3.06, 26.24, -31.5 kJ/mole for n= 0,..., 5, respectively. The laterally interaction between SAM molecules and gold surface was described by the Lennard-Jones 12-3 potential. (Tupper & Brenner 1994)

$$U = \sum_{\text{SAM-Au}} 2.117\varepsilon_{ij}\left[\left(\frac{\sigma_{ij}}{r_{ij}}\right)^{12} - \left(\frac{\sigma_{ij}}{r_{ij}}\right)^{3}\right] \tag{3}$$

The gold atoms were restricted on the positions of the lattice points in the substrate. Water molecules were explicitly considered and were modeled by extended simple point charge (SPC/E) model. (Berendsen et al. 1987)

The hydrophobic interaction was the main interaction between CTX and SAM. The enthalpic and entropic components of the hydrophobic interaction were correctly involved and treated once the water molecules were explicitly modeled in our studies. Since the SAM molecules in the current study carry no charge, the potential energy between SAM and the other molecules was vdW interaction and the parameters were determined by the geometrical combination rule.

2.3 Initial configuration

It has been reported that phase separation can take place when SAM was composed of components of different terminal groups such as 3-mercaptopropanol and *n*-tetradecanethiol, *n*-undecanethiol and 11-mercaptoundecanoic acid, 3-mercapto-*N*-nonylpropionamide and *n*-decanethiol and so on. (Smith et al. 2004) However, for SAM composed of the components of similar terminal groups, phase separation, in general, did not happen. For example, Whitesides and coworkers had done a series of experimental studies on methyl-terminated mixed SAM systems (Laibinis et al. 1992; Folkers et al. 1992; Bain & Whitesides 1989) and shown that chain length difference in the SAM did not render the systems into the formation of macroscopic islands. Using atomic force microscope imaging, other group (Tamada et al. 1997) also reported no phase separation in the mixed SAMs composed of $S(CH_2)_3CH_3$ and $S(CH_2)_{17}CH_3$. A recent review summarized again that molecules of similar composition did not phase separate in a SAM system formed from solutions at room temperature. (Smith et al. 2004) The results indicated that the mixed SAMs were not macroscopically phase separated according to Folkers *et al.* (Folkers et al. 1992) Based upon the above information, a homogenous mixture of the simulated SAM systems was assumed and the SAM surfaces were generated by randomly placing C5 and C9 molecules on the gold substrate in the present simulations.

The initial configuration of the CTX protein was prepared in the way with the three CTX finger loops facing the SAM surface. This orientation had been confirmed as the most favorable orientation of CTX proteins binding to membrane by experiments from Wu's group. (Forouhar et al. 2003; Huang et al. 2003) Efremov *et al.* (Efremov et al. 2004) and Lomize *et al.* (Lomize et al. 2006) obtained the same result by using MC method and transfer energy minimization method respectively. Therefore, the initial configuration with the three finger loops of the CTX facing down was set to facilitate the adsorption of the system to the truly favorable orientation for the present simulations.

2.4 Simulation procedure

After generating the initial configurations, the systems were solvated in a bath of water molecules with a density of 1 g/cm^3. One Na^+ ion and ten Cl^- ions were added into the simulation box to maintain the electro-neutrality of the systems. The simulation box was a rectangular parallelepiped of 5.99 × 5.19 × 10.00 nm^3 with periodic boundary conditions applied in the *x* and *y* directions. The *z* direction was restricted by a wall (cf. Fig.1). The velocities were initially assigned to each atom with a Maxwell-Bolzmann distribution at 50 K. The system was then gradually heated to 300 K in a period of 400 ps to initially relax the water molecules around the protein and the SAM surface.

The annealing process (Kirkpatrick et al. 1983) was then performed to overcome local minima and search the global minimum of energy landscape of the interaction between CTX and SAM. The process was started by an initial heating stage in which the system was heated from 300 to 350 K. The temperature was then maintained at 350 K for 400 ps, followed by a slow cooling at a rate of 0.1 K/ps to 300 K. 300 K was then maintained for 4 ns until the interaction energy between CTX and SAM reached a constant value. The simulations were performed in canonical ensemble with the integrating time step equal to 1.0 fs. The temperature was controlled by Berendsen thermostat (Berendsen et al. 1984) with the time constant equal to 0.1 ps in the annealing process and then the temperature was controlled by a Nose-Hoover thermostat. (Hoover 1985; Nose 1984) Because bond vibration is very fast, all the covalent bonds were constrained by the LINCS algorithm. (Hess et al. 1997) For the nonbonded interactions, the cutoff distance was chosen to be 1.5 nm for the vdW interaction. The Coulomb interaction was cut at 2.5 nm by a force-shifting function. It has been demonstrated (Steinbach & Brooks 1994) that the cutoff method for the electrostatic interaction can correctly model the dynamics of biomolecules in solutions. The twin-range approach in neighbor searching (Wilfred F. van Gunsteren and Herman J. C. Berendsen 1990) was performed, with short range distance equal to 1.5 nm and long range distance equal to 2.5 nm. Data were saved every 1.0 ps for analysis. All the simulations were performed using the program GROMACS. (Van Der Spoel et al. 2005) The simulation snapshots were plotted using the software PyMOL. (DeLano 2002)

2.5 Steered molecular dynamic simulations

In our study (Hung et al.2011), SMD simulated the pulling process of CTX adsorbed on the SAM surface by applying an external force to the CTX molecule, and it monitored the adsorption force and structural change of the CTX molecule during the desorption process. Before the pulling process started, the model system was in equilibrium, and the CTX molecule was adsorbed onto the SAM surface. The equilibrium state was kept at 300 K for an additional 3 ns. The starting configurations of the model system for SMD simulations were generated by extracting configurations from the last nanosecond of the equilibrium stage.

In the pulling process during the SMD simulation, external forces were applied to the CTX through the center of mass to pull the CTX off of the SAM surface with a constant velocity perpendicular to the SAM surface (i.e., *z* direction in Fig. 1). The adsorption force *f* at time *t* can be represented by the following equation

$$f(t) = k[(Z_{CTX,0} + vt) - Z_{CTX}(t)] \tag{4}$$

where k is the force constant, v is the pulling velocity and $Z_{CTX}(t)$ and $Z_{CTX,0}$ are the z coordinates of CTX at time t and initial time 0, respectively. In our study, we defined Z as the distance from gold substrate, i.e., Z=0 is the position of the gold.

The stiff-spring approximation (Park & Schulten 2004; Park et al. 2003) with a large force constant was applied to minimize the fluctuation of reaction coordinate among different trajectories. The approximation was valid only if the force constant was sufficiently larger than the curvature of the energy landscape at its minimum, which was approximately the maximum of the second derivative of PMF profile. (Hummer & Szabo 2010) However, the fluctuations of applied force were related to k through $(k_BTk)^{1/2}$,where k_B was the Boltzmann's constant and T was the absolute temperature, and thus the force constant cannot be arbitrarily large. (Balsera et al. 1997) In our study, the force constant was chosen to be 1209 k_BT/nm^2, which was four times as large as the maximum of the second derivative of PMF profile calculated using the umbrella sampling method, to ensure the validity of the stiff-spring approximation. The total traveling distance was up to 2 nm starting from Z_{CTX}=2.0 nm, which was the equilibrium position of CTX protein adsorbed on the SAM surface, to Z_{CTX}=4.0 nm, where the separation distance was far enough that there was no interaction between the CTX protein and SAM surface.

2.6 PMF calculation

PMF is a potential along a reaction coordinate, the gradient of which yields the negative of the average force acting on the targeted molecule over all the configurations at a given place. Physically, PMF represents the difference of free energy, ΔF, along the coordinate of reaction. In statistical physics, the difference ΔF between two coordinates z and z_0, can be calculated by the ratio of the two configurational integrals as follow:

$$\Delta F = F(z) - F(z_0) = -\frac{1}{\beta}\ln\frac{\int d^{3N-1}\,\mathrm{Rexp}[-\beta U(z,\mathbf{R})]}{\int d^{3N-1}\,\mathrm{Rexp}[-\beta U(z_0,\mathbf{R})]} \tag{5}$$

where z is the reaction coordinate, z_0 is the reference position, **R** denotes the remaining $3N$-1 coordinates, U(z,**R**) is the system potential, and $\beta=1/k_BT$ with k_B being the Boltzmann's constant and T the absolute temperature.

In the circumstance of equilibrium MD simulations without applying external potentials, the regions with large PMF are not easily explored because the large difference of free energy hinders the access of the target molecule into the regions. It is hence difficult to calculate numerically the configurational integral over such regions with good accuracy. To overcome the problem, calculation methods for PMF had been devolped and classified as either equilibrium or non-equilibrium approaches.(Ytreberg et al. 2006) The equilibrium approaches, i.e. the umbrella sampling method, (Torrie & Valleau 1977) and the non-equilibrium approaches, i.e. using Jarzynski's remarkable equality (Jarzynski 1997) from SMD simulations. Further comparisons and details of these two approaches are given in our previous study. (Hung et al. 2011)

3. Results and discussions

The results and discussions were summarized in two parts. In the first part, the influence of different solvent models on the systems was investigated at first. The results demonstrated

that to include water molecules explicitly was crucial in the study of the protein adsorption. Therefore, the explicit water model was implemented to study the protein adsorption on SAMs of different mixing ratios (χ_{C9}). The binding energies were obtained by means of MD simulations. The binding energy was studied by calculating the nonbonded interactions of the protein with the SAM surface. The CTX/SAM contact area and the structure of SAM molecules were examined to investigate the binding enhancement of the CTX protein adsorbing onto a SAM surface. Other physical mechanisms were discussed in our previous study. (Hung et al. 2010) In the second part, the dynamic information including the structural changes, adsorption forces a CTX protein desorbed from the pure C5 SAM surface were monitored in the SMD simulation. The thermodynamic information, PMF, was calculated using the umbrella sampling method for better interpretation of the CTX desorption process.

3.1 Static properties of CTX adsorption

3.1.1 Comparison of results using different solvent models

There have been many alternative solvent models proposed to minimize the requirement of computer resources in simulating water. (Smith & Pettitt 1994) For example, the distance-dependent dielectric function was a model widely used in many studies. To demonstrate the importance of the role of water in the adsorption of CTX on SAM, we performed the simulations using the distance-dependent dielectric model to simulate water environment. In this model, solvent molecules were not explicitly treated but implicitly considered together as a dielectric continuum. The dielectric constant was set to 1 within a cut-off distance (2.5 nm), and 78 beyond the cut-off distance. The binding energy of CTX on SAM calculated from the distance-dependent dielectric model showed the similar trend of behavior as from the explicit water model, but the error bar of data was larger for the distance-dependent dielectric model (Fig. 2). Therefore, the CTX protein in the distance-dependent dielectric model displayed a different conformation, compared to in the explicit water model. Fig. 3 showed snapshots of an equilibrium conformation of the CTX protein on the χ_{C9} = 0.5 SAM surface obtained from the two models. We observed that the CTX protein was almost lying flat on the SAM surface for the distance-dependent dielectric model. The orientation was different from the one by the explicit water model. Thus, higher binding

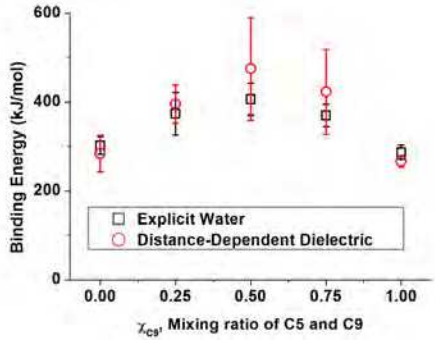

Fig. 2. Binding energy of CTX to SAM surfaces of different mixing ratios in the distance-dependent dielectric model and in the explicit solvent model. (Hung et al. 2010)

energy was obtained for the former model due to the larger contact area. In the distance-dependent dielectric model, there was no water molecule on the CTX-SAM interface to prevent direct contact of CTX and SAM and hence the interaction between them was so strong that the conformation of the CTX protein was largely deformed and the orientation was not in agreement with experimental observations. With explicit water molecules, the entropic component of the hydrophobic effect was considered and thus the hydrophobic effect induced some kinds of ordering in the surrounding water. More precisely, the hydrophilic residues of CTX were solvated by the water molecules via the hydrogen bonding. As a consequence, the CTX molecule was adsorbed on the SAM surface with specific orientation. The results demonstrated that to include water molecules explicitly in the model was crucial in the study of the protein adsorption. The binding mechanisms and protein conformation can be correctly identified only when it was considered.

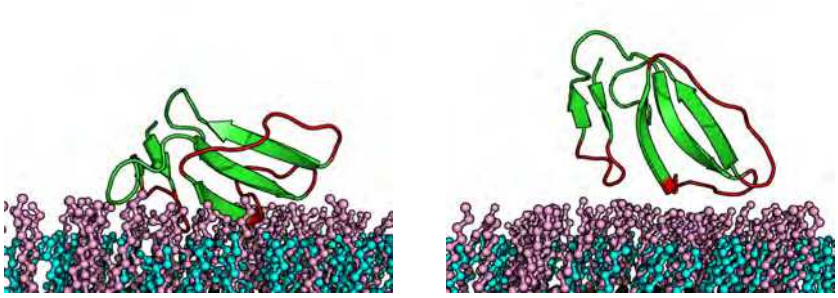

(a) (b)

Fig. 3. Snapshots of CTX on χ_{C9} = 0.5 SAM surface using different solvent models: (a) distance-dependent dielectric model; (b) explicit solvent model. (Hung et al. 2010)

3.1.2 Binding energy of a CTX protein on SAM surface

The affinity of a CTX protein on SAM surface was of interest. This affinity can be quantified by calculating the binding energy between CTX and SAM, which was the sum of all the non-bonded interactions between them. Fig. 4 showed a maximum in the middle. The binding energy of the CTX protein to the pure C5 and the energy to the pure C9 SAM surfaces were similar to each other but significantly smaller than that to a mixed SAM surface. The enhancement of the binding energy on a mixed SAM surface can be as large as 34% when χ_{C9} = 0.5.

3.1.3 Physical mechanisms of CTX adsorption

The enhancement of the binding energy can be explained by the equilibrium configurations of CTX landing on SAM surfaces composing of different mixing ratios as shown in Fig. 5. In the pure C5 and C9 SAM systems, the surface roughness is small. The CTX protein landed stably on the flat surface and the conformation of the CTX looked similarly to each other. On the other hand, the surface roughness was increased in the mixed SAM systems. The three-finger loops of the CTX can penetrate into the region between C5 and C9 molecules, especially when χ_{C9} = 0.25 and 0.5, resulting in the increase of the CTX-SAM contact area.

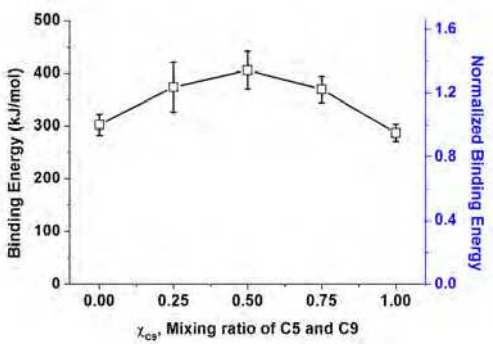

Fig. 4. Binding energy (read from left) of CTX adsorded on SAM surfaces of different mixing ratios, χ_{C9}. The normalized binding energy (read from right) is calculated by dividing the binding energy by the value on the C5 SAM surface. (Hung et al. 2010)

The CTX-SAM contact area and the structure of SAMs were described in the following sections.

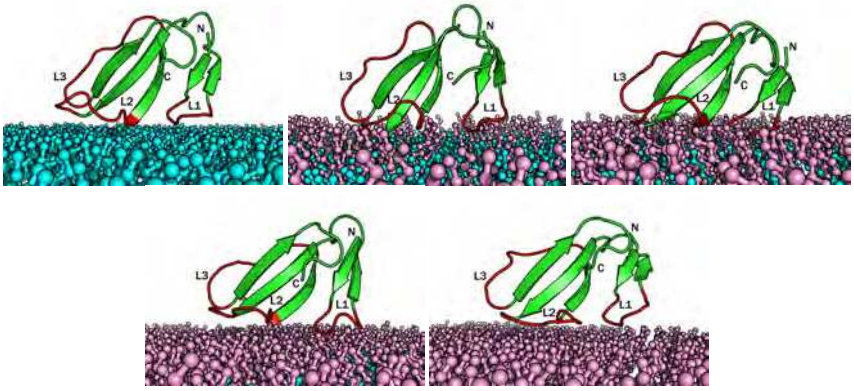

Fig. 5. Snapshots of CTX on (a) χ_{C9} = 0, (b) χ_{C9} = 0.25, (c) χ_{C9} = 0.5, (d) χ_{C9} = 0.75, and (e) χ_{C9} = 1 SAM surface. Water molecules are not shown in the figures to provide clear illustrations of the protein configurations. (Hung et al. 2010)

It was commonly accepted that the free-energy change of protein from water to membrane was proportional to the change of area contacting with the surrounding water area of protein. (White & Wimley 1994; Reynolds et al. 1974; Eisenberg & McLachlan 1986) This idea was extended to our system and verified if the binding energy of CTX on SAM also followed a linear relation against the CTX-SAM contact area. The area was calculated by the method of double cubic lattice (Eisenhaber et al. 1995) with a probe radius equal to 0.14 nm. The result of the binding energy versus the contact area was plotted in Fig. 6. It showed that the binding energy satisfied a linear equation with the surface area of CTX in contact with the SAM surface. The slope of the linear equation was 36.05 kJ/mol·nm^2. Therefore, the binding energy was higher on the mixed SAMs surface than on the pure SAM. Mixed SAMs surfaces were rough surfaces which increased the contact area.

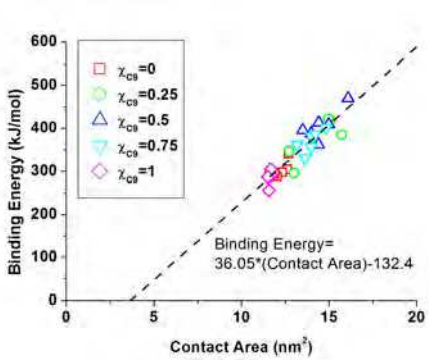

Fig. 6. Binding energy as a function of CTX-SAM contact area. (Hung et al. 2010)

Since the binding energy was strongly related to the CTX-SAM contact area, the structure of the SAM molecules can be another important factor in determining the protein adsorption. Mixed SAMs can be divided to two layer regions as observed by Bain, (Bain & Whitesides 1989) illustrated in Fig. 7(a). The first layer region was the inner region adjacent to the gold substrate and the second one was the outer layer in contact with the solution. The mobility of the SAM molecules can be calculated by the root mean square deviation (RSMD) of the alkanethiol chains in the SAM in a time interval equal to 1 ps. The larger the RMSD, the higher the mobility would be. Fig. 7(b) showed that the RMSD of the C5 surface was higher than that of the C9 surface, which showed a better ordering when the chain length was long.

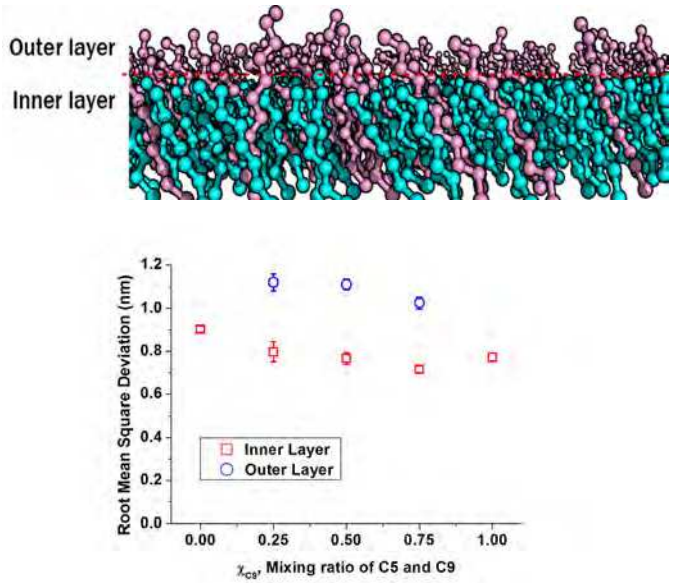

Fig. 7. (a) Illustion of inner and outer layers for mixed SAM surfaces; (b) Root mean square deviations for inner and outer layers versus mixing ratio χ_{C9} of SAM surface. (Hung et al. 2010)

The chain length dependence had been studied by experiments. (Fenter et al. 1997; Porter et al. 1987) These experiments showed that there existed distinct differences in structure between long-chained and short-chained SAMs. The long-chained SAMs formed a densely packed, crystalline-like structure while the structures of the short-chained SAMs became increasingly disordered. The results were consistent with the experiments. The large number of methylene groups in the long-chained SAM provided a strong vdW interaction to sustained an ordered structure. On the other hand, for the mixed SAM surfaces, the RMSD value was larger in the outer layer region than in the inner one. This was in agreement with the Bain's study, which showed that the inner layer packed better than the outer one.

The mixture of alkanethiols of different chain lengths in the SAM provided an additional dimension of the reaction area, especially for the hydrophobic interaction, on the limited surface. As a result, the CTX affinity was enhanced on the mixed SAM surface. In order to investigated the relation between the CTX binding and the SAM surface area, the SAS area of the mixed SAMs surface was calculated and plotted in Fig. 8. It showed that the CTX-SAM contact area was highly correlated to the SAM surface area. The result suggested that the three dimensional nanostructured morphology, due to the chain length difference of the alkanethiol chains in SAM, promoted the contact of CTX protein on the SAM surface.

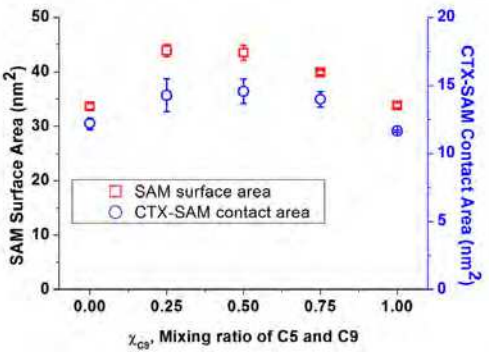

Fig. 8. SAM surface area and CTX-SAM contact area versus mixing ratio χ_{C9} of SAM surface. (Hung et al. 2010)

3.2 Dynamic information of CTX desorption process

3.2.1 Structural changes of CTX during the desorption process

CTX is a highly stable protein due to the presence of four disulfide bonds and a core of hydrophobic residues. (Sivaraman et al. 1998) As a result, the CTX protein does not undergo unfolding during desorption processes. SMD simulations provided dynamic structure histories of the CTX protein during the pulling process, and the key CTX molecular conformations were shown in Figs. 9(a)-9(d) for a pulling velocity of 0.25 nm/ns. The structural change of the CTX protein during the desorption process was due to these three loops. Starting from the equilibrium orientation of the three-finger loops facing and attached to the SAM surface (Fig. 9(a)), when CTX was pulled from the surface at a constant velocity, Loop I's tip detached from the surface first (Fig. 9(b)), and Loops II and III detached later at

about the same time (Fig. 9(c)) before the entire protein was detached from the surface (Fig. 9(d)). The correlation between the trajectories of the three loops' tips ($Z_{Loop,i}$) and of the center of mass of protein (Z_{CTX}) from the gold substrate can quantitatively indicated the structural changes of the CTX protein during the desorption process, as shown in Fig. 9(e). The centers of mass of three amino acid residues, Val7, Ala28, and Leu47, were chosen to represent the tip positions of the three loops, $Z_{Loop\ I}$, $Z_{Loop\ II}$, and $Z_{Loop\ III}$, respectively. The average position of the methyl groups of the SAMs was about 1.0 nm from the gold substrate, and the vdW radius of methyl group was ~0.2 nm. (A J Li and Nussinov 1998) Thus, all three $Z_{Loop,i}$ were about 1.3~1.4 nm from the gold substrate when the loop contacted the SAM surface. It was reasonable to define that the i^{th} loop tip detached from the SAM surface when $Z_{Loop,i}$ was larger than 1.6 nm**.** In general, the desorption process can be described in three stages as follows: in the first stage, CTX contacted the SAM surface with the three loops attached until Loop I detached from the SAM surface at Z_{CTX}~2.3-2.4 nm, and $Z_{Loop,i}$<1.6 nm for all three loops i=1, 2, and 3. In the second stage, Loop I rose with Z_{CTX} while Loops II and III remained in contact with the SAM surface, and $Z_{Loop,i}$<1.6 nm for i=2 and 3 only. Loops II and III detached from the SAM surface almost at the same time at Z_{CTX}~3.3 nm. The three loops were far from the SAM surface in the third stage.

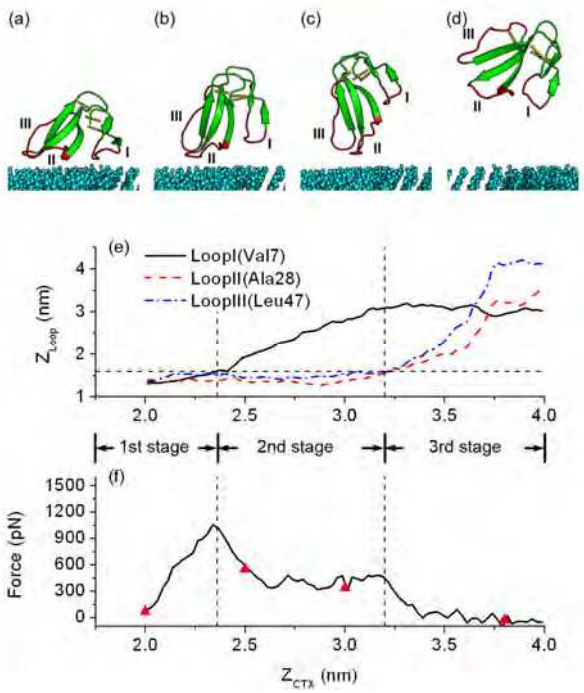

Fig. 9. (a)-(d) CTX conformations at Z_{CTX}=2.0, 2.5, 3.0, and 3.8 nm, respectively. (e) Z_{Loop}, positions of the three loop tips of CTX (black solid line: LoopI; red dashed line: LoopII; blue dashed-dotted line: LoopIII) and (f) adsorption force vs. Z_{CTX}, center of mass of CTX, when pulling with velocity v=0.25 nm/ns. Red triangles mark the positions of the snapshots in (a)-(d). (Hung et al. 2011)

3.2.2 Adsorption force during the desorption process

The adsorption forces and structural changes of the CTX protein during the desorption process from the SAM surface were the important results of the SMD simulation. Fig. 9(f) shows the adsorption force of the CTX protein as it was pulled with a constant velocity of 0.25 nm/ns. Three stages can be distinguished from the force curve. In the first stage, the force was monotonically rising until it reached a peak, i.e., the rupture force in the present study at Z_{CTX}~2.3-2.4 nm. The force then decreased to a plateau in the second stage for 2.5 nm< Z_{CTX}<3.2 nm, and the force diminishes to nearly zero in the third stage (Z_{CTX}>3.2 nm). These stages were closely correlated when the loops were either attached or detached.

Summarizing the history of the adsorption force and positions of the three loop tips, $Z_{Loop,i}$, the desorption process can be described in three stages. In the first stage, the adsorption force increased with Z_{CTX} until it was large enough to break Loop I from the SAM surface. In the second stage, the CTX-SAM was in a quasi-equilibrium state with Loops II and III contacting the SAM surface, and thus, the force remained constant in this stage. In the third stage, CTX was located far enough from the SAM surface that there was no interaction force between the CTX and SAM surface. The detachment of Loop I from the SAM surface gave the rupture force, which suggested that Loop I played an important role in the CTX desorption process from the SAM surface. This observation agreed with two-dimensional NMR spectroscopy experiments, (Sivaraman et al. 2000) which had shown that Loops II and III were more stable than Loop I. Hence, Loop I possessed the highest flexibility of the three loops, which was related to its biological activity. As it had the highest flexibility, Loop I should be the first loop to pull off from the surface, which was consistent with the SMD simulation results.

Different pulling velocities leading to different hysteresis effects (Liphardt et al. 2001) and different rupture forces (Liphardt et al. 2002) were observed in the previous studies. In the present simulations, the desorption processes at pulling velocities of v=1.0 nm/ns and v=0.25 nm/ns were qualitatively consistent with the three distinguished stages. However, three major differences were observed: the magnitude of the adsorption force at a higher pulling velocity was much higher than that at a lower pulling velocity, the quasi-equilibrium state was indeterminate and the adsorption force was not diminished when the CTX was far from the SAM surface at v=1.0 nm/ns. These distinctions were a result of the pronounced non-equilibrium phenomena, such as friction and dissipation, at high pulling velocity. Furthermore, it was noted that the orientation of CTX in the bulk solvent environment at higher pulling velocity (Fig. 10(d)) was similar to that of CTX just departing from the SAM surface (Fig. 10(c)). There was no specific orientation of CTX in the bulk solvent environment at a lower pulling velocity (Figs. 9(c) and 9(d)), which implies that CTX was not relaxed with the surrounding molecules at a high pulling velocity of v=1.0 nm/ns.

To depict the adsorption force-pulling velocity dependence, the averaged force curves at four different pulling velocities were shown in Fig. 11(a). The force curves were in qualitative agreement by shape, but the magnitude of the peak adsorption force and the width of the second plateau-like stage were different at different pulling velocities. Because the difference between the forces at v=0.125 nm/ns and at 0. 25 nm/ns was very small and the computation time for the v=0.125 nm/ns case was twice that of the v=0.25 nm/ns case, the major computations were conducted at v=0.25 nm/ns for the present study. Figure 11(b) showed that the average rupture force was related to the pulling velocity in terms of the

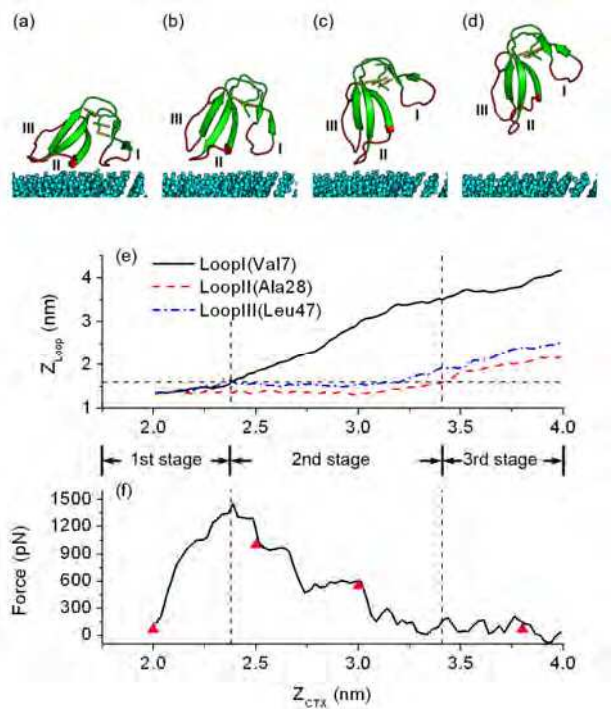

Fig. 10. (a)-(d) CTX conformations at Z_{CTX}=2.0, 2.5, 3.0, and 3.8 nm, respectively. (e) Z_{Loop}, positions of the three loop tips of CTX (black solid line: LoopI; red dashed line: LoopII; blue dashed-dotted line: LoopIII) and (f) adsorption force vs. Z_{CTX}, center of mass of CTX, when pulling with velocity v=1.0 nm/ns. Red triangles mark the positions of the snapshots in (a)-(d). (Hung et al. 2011)

linear (green dash-dotted line) and logarithmic (red dash line) fittings. Some SMD studies (Sotomayor & Schulten 2007; Gao et al. 2002) found that the rupture force values are increased logarithmically with the pulling velocities, while other studies (Heymann & Grubmüller 1999; Marrink et al. 1998) found the linear dependence on the pulling velocities for high pulling velocities. The behavior between the rupture force and pulling velocity can be described well in terms of both linear and logarithmic relationships for pulling velocity ranging from 0.125 nm/ns to 1.0 nm/ns in our SMD simulations. The near-linear correlation indicated that the desorption process was within the friction force-dominated regime for the present study.

3.2.3 PMF calculated by the umbrella sampling method

Because the pulling forces depended strongly on the pulling velocity, further information of the CTX desorption process can be obtained from the free energy landscape, i.e., PMF. The resulting PMF profile from the umbrella sampling (Fig. 12(a)) showed a sharp change of the slope at Z_{CTX}~2.5 nm, a subsequent gradual increase afterward (2.5 nm <Z_{CTX}<3.2 nm), and a plateau after Z_{CTX}~3.2 nm. The sharp change indicated a free energy barrier at Z_{CTX}~2.5 nm.

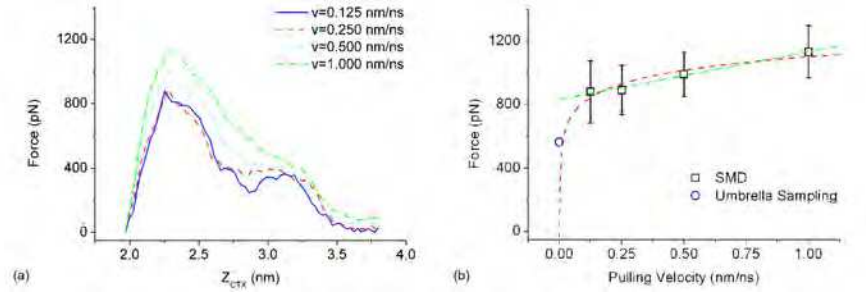

Fig. 11. (a) Average adsorption force curves with various pulling velocities, i.e., v=0.125 (blue solid line), 0.25 (red dashed line), 0.5 (cyan dotted line), and 1 nm/ns (green dashed-dotted line). (b) Average rupture force vs. pulling velocity from SMD simulations (squares). Blue circle indicates the rupture force obtained from the derivation of the PMF calculated using umbrella sampling. The green dashed-dotted and red dashed lines represent the best linear and logarithm fits to the average rupture forces, respectively. (Hung et al. 2011)

For comparison with the pulling force curves from SMD simulations, the mean force profile was obtained from the derivative of the PMF profile with respect to Z_{CTX} (Fig. 12(b)). A remarkable agreement between the mean force (Fig. 12(b)) and SMD force-distance curves (Fig. 9(f) and Fig. 10(f)) was obtained.

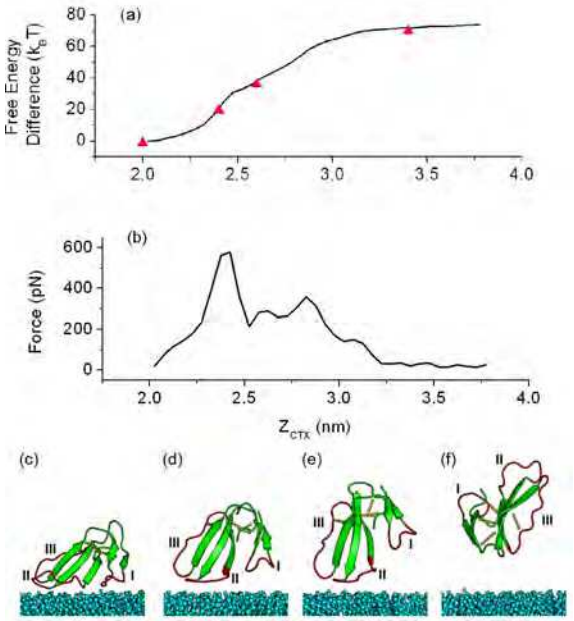

Fig. 12. (a) PMF profile calculated using umbrella sampling. Red triangles mark the positions of the snapshots in (c)-(f). (b) Mean force profile obtained from the derivative of the PMF with respect to Z_{CTX}. (c)-(f) CTX conformations at Z_{CTX} =2.0, 2.4, 2.7, and 3.4 nm, respectively. (Hung et al. 2011)

The adsorption force from the SMD simulation included the random force, friction force, and thermodynamic force, but he mean force from the umbrella sampling method represented the thermodynamic force between the CTX protein and the SAM surface. Similar force-distance curves and similar structural changes impled cross-validation and also capture key features of the process from both approaches. Furthermore, the peak forces of both force-distance curves occurred at the same departing distance, Z_{CTX}~2.5 nm, indicating that the departure of the first loop was a major rupture force in the desorption process and the use of a pulling force from SMD that was higher than the mean force from the umbrella sampling was reasonable. For the range of pulling velocities applied in SMD simulations, the friction force played a role in the adsorption force, and thus, the relationship between the adsorption force and pulling velocity was near-linear at higher pulling velocities. However, the relationship between the adsorption force and pulling velocity becomes logarithmic with lower pulling velocities for the thermodynamic force-dominated regime. (Marrink et al. 1998) As a result, the mean force (blue circle in Fig. 12(b)) cannot be achieved by extrapolating linearly to zero pulling velocity. Instead, the SMD data might approach the mean force by logarithmically extrapolating to zero pulling velocity, as shown in Fig. 12(b).

4. Conclusion and prospects

In the present study, the adsorption of CTX proteins on alkanethiol SAMs of different mixing ratios was analyzed by means of MD simulations. Different solvent models had been examined and the results demonstrated that the use of explicit water molecules was necessary to correctly take into account the enthalpic and entropic components of the hydrophobic effect when one studies protein adsorption on SAMs. The results showed that the binding energy has the highest value when χ_{C9} was 0.5 and were in good agreement with the experimental data. Moreover, the binding energy between CTX and SAM surface was proportional to the CTX-SAM contact area. The structure of SAMs molecules determined the CTX-SAM contact area, and hence the binding energy.

Dynamic information, such as structural change and adsorption force, about the desorption of a single CTX protein from a SAM surface was investigated by means of SMD simulations successfully. The simulation results indicated that CTX did not undergo unfolding during the pulling process and Loop I was the first loop to depart from the SAM surface. This observation was in good agreement with the results of the NMR spectroscopy experiment. For the pulling velocity ranging from 0.125 nm/ns to 1.0 nm/ns employed in the present study, the near-linear dependence of force on pulling velocity indicated that the friction force played a significant role in the force measured in SMD simulations. A remarkable agreement was obtained between the force-distance interaction from the umbrella sampling method and the pulling force-distance curve from SMD, which cross-validated these techniques and also captured the same key features of the process from both approaches. Furthermore, the peak forces of both force-distance curves occurred at the same departing distance, Z_{CTX}~2.5 nm, indicated that the departure of the first loop was resulted in the major rupture force in the desorption process. The results provided valuable information at atomic level toward a fundamental understanding of protein adsorption.

Future work will focus on the PMFs calculation of CTX adsorption on mixed SAMs of different mixing ratios. It will provide key features for enhacing protein adsorption or protein resistance on the designed surface by manipulating the mixing ratios.

5. Acknowledgment

The authors thank the National Center for High-Performance Computing, Taiwan for computing resources and the National Science Council, Taiwan for financial support under Grant (NSC99-2221-E007-028-MY2).

6. References

Agashe, M.; Raut, V.; Stuart, S. J. & Latour, R. A. (2005). Molecular Simulation to Characterize the Adsorption Behavior of a Fibrinogen Gamma-Chain Fragment. *Langmuir*, Vol.21, No.3, pp. 1103-1117

Bain, C.D. & Whitesides, G. M. (1989). Formation of Monolayers by the Coadsorption of Thiols on Gold: Variation in the Length of the Alkyl Chain. *Journal of the American Chemical Society*, Vol.111, No.18, pp. 7164-7175

Balsera, M.; Stepaniants, S.; Izrailev, S.; Oono, Y. & Schulten, K. (1997). Reconstructing Potential Energy Functions from Simulated Force-Induced Unbinding Processes. *Biophysical Journal*, Vol.73, No.3, pp. 1281-1287

Berendsen, H. J. C., Grigera, J. R. & Straatsma, T. P. (1987). The Missing Term in Effective Pair Potentials. *The Journal of Physical Chemistry*, Vol.91, No.24, pp. 6269-6271

Berendsen, H. J. C.; Postma, J. P. M.; Gunsteren, W. F. van; DiNola, A. & Haak, J. R. (1984). Molecular Dynamics with Coupling to an External Bath. *The Journal of Chemical Physics*, Vol.81, No.8, pp. 3684-3690

Chandler, D. (2005). Interfaces and the Driving Force of Hydrophobic Assembly. *Nature*, Vol.437, No.7059, pp. 640-647

Dauplais, M.; Neumann, J. M.; Pinkasfeld, S.; Ménez, A. & Roumestand, C. (1995). An NMR Study of the Interaction of Cardiotoxin Gamma from Naja Nigricollis with Perdeuterated Dodecylphosphocholine Micelles. *European Journal of Biochemistry / FEBS*, Vol.230, No.1, pp. 213-220

DeLano, W. L. (2002). The PyMOL Molecular Graphics System. , Available from http://www.pymol.org

Dubovskii, P. V.; Lesovoy, D. M.; Dubinnyi, M. A.; Konshina, A. G.; Utkin, Y. N.; Efremov, R. G. & Dubovskii, A. S. A. (2005). Interaction of Three-Finger toxins with Phospholipid Membranes: Comparison of S- and P-Type Cytotoxins. *The Biochemical Journal*, Vol.387, No.Pt 3, pp. 807-815

Dufton, M. J. & Hider, R. C. (1988). Structure and Pharmacology of Elapid Cytotoxins. *Pharmacology & Therapeutics*, Vol.36, No.1, pp. 1-40

Efremov, R. G.; Nolde, D. E.; Konshina, A. G.; Syrtcev, N. P. & Arseniev, A. S. (2004). Peptides and Proteins in Membranes: What can We Learn via Computer Simulations? *Current Medicinal Chemistry*, Vol.11, No.18, pp. 2421-2442

Eisenberg, D. & McLachlan, A. D. (1986). Solvation Energy in Protein Folding and Binding. *Nature*, Vol.319, No.6050, pp. 199-203

Eisenhaber, F.; Lijnzaad, P.; Argos, P.; Sander, C. & Scharf, M. (1995). The Double Cubic Lattice Method: Efficient Approaches to Numerical Integration of Surface Area and Volume and to Dot Surface Contouring of Molecular Assemblies. *Journal of Computational Chemistry*, Vol.16, No.3, pp. 273-284

Fenter, P.; Eberhardt, A.; Liang, K.-S. & Eisenberger, P. (1997). Epitaxy and Chainlength Dependent Strain in Self-Assembled Monolayers. *The Journal of Chemical Physics*, Vol.106, No.4, pp. 1600-1608

Folkers, J. P.; Laibinis, P. E. & Whitesides, G. M. (1992). Self-Assembled Monolayers of Alkanethiols on Gold: Comparisons of Monolayers Containing Mixtures of Short- and Long-Chain Constituents with Methyl and Hydroxymethyl Terminal Groups. *Langmuir*, Vol.8, No.5, pp. 1330-1341

Forouhar, F.; Huang, W.-N.; Liu, J.-H.; Chien, K.-Y.; Wu, W.-g. and Hsiao, C.-D. (2003). Structural Basis of Membrane-Induced Cardiotoxin A3 Oligomerization. *The Journal of Biological Chemistry*, Vol.278, No.24, pp. 21980-21988

Gao, M.; Lu, H. & Schulten, K. (2002). Unfolding of Titin Domains Studied by Molecular Dynamics Simulations. *Journal of Muscle Research and Cell Motility*, Vol.23, No.5-6, pp. 513-521

Gore, J.; Ritort, F. & Bustamante, C. (2003). Bias and error in estimates of equilibrium free-energy differences from nonequilibrium measurements. *Proceedings of the National Academy of Sciences of the United States of America*, Vol.100, No.22, pp. 12564-12569

Gray, J. J. (2004). The Interaction of Proteins with Solid Surfaces. *Current Opinion in Structural Biology*, Vol.14, No.1, pp. 110-115

Hautman, J. & Klein, M. L. (1989). Simulation of a Monolayer of Alkyl Thiol Chains. *The Journal of Chemical Physics*, Vol.91, No.8, pp. 4994-5001

Hess, B.; Bekker, H.; Berendsen, H. J. C. & Fraaije, J. G. E. M. (1997). LINCS: A Linear Constraint Solver for Molecular Simulations. *Journal of Computational Chemistry*, Vol.18, No.12, pp. 1463-1472

Heymann, B. & Grubmüller, H. (1999). AN02/DNP-Hapten Unbinding Forces Studied by Molecular Dynamics Atomic Force Microscopy Simulations. *Chemical Physics Letters*, Vol.303, No.1-2, pp. 1-9

Hoover, W. G. (1985). Canonical Dynamics: Equilibrium Phase-Space Distributions. *Physical Review A*, Vol.31, No.3, pp. 1695–1697

Hower, J. C.; He, Y.; Bernards, M. T. & Jiang S. (2006). Understanding the Nonfouling Mechanism of Surfaces through Molecular Simulations of Sugar-Based Self-Assembled Monolayers. *The Journal of Chemical Physics*, Vol.125, No.21, pp. 214704

Huang, W.-N.; Sue, S.-C.; Wang, D.-S.; Wu, P.-L. & Wu, W.-g. (2003). Peripheral Binding Mode and Penetration Depth of Cobra Cardiotoxin on Phospholipid Membranes as Studied by a Combined FTIR and Computer Simulation Approach. *Biochemistry*, Vol.42, No.24, pp. 7457-7466

Hummer, G. & Szabo, A. (2010). Free Energy Profiles from Single-Molecule Pulling Experiments. *Proceedings of the National Academy of Sciencess of the United States of America*, Vol.107, No.50, pp. 10-15.

Hung, S.-W.; Hsiao, P.-Y. & Chieng, C.-C. (2011). Dynamic Information for Cardiotoxin Protein Desorption from a Methyl-Terminated Self-Assembled Monolayer Using Steered Molecular Dynamics Simulation. *The Journal of Chemical Physics*, Vol.134, No.19, pp. 194705

Hung, S.-W.; Hsiao, P.-Y. & Chieng, C.-C. (2010). Mixed-SAM Surfaces Monitoring CTX-protein, part II: Analysis using Molecular Dynamics Simulations. *IEEE Transactions on Nanobioscience*, Vol.9, No.4, pp. 297-306.

Hung, S.-W.; Hwang, J.-K.; Tseng, F.; Chang, J.-M.; Chen, C.-C. & Chieng, C.-C. (2006). Molecular Dynamics Simulation of the Enhancement of Cobra Cardiotoxin and E6 Protein Binding on Mixed Self-Assembled Monolayer Molecules. *Nanotechnology*, Vol.17, No.4, pp. S8-S13.

Isralewitz, B.; Gao, M. & Schulten, K. (2001). Steered Molecular Dynamics and Mechanical Functions of Proteins. *Current Opinion in Structural Biology*, Vol.11, No.2, pp. 224-230.

Jarzynski, C. (1997). Nonequilibrium Equality for Free Energy Differences. *Physical Review Letters*, Vol.78, No.14, pp. 2690-2693

Kirkpatrick, S.; Gelatt, C. D. & Vecchi, M. P. (1983). Optimization by Simulated Annealing. *Science*, Vol.220, No.4598, pp. 671-680

Kirkwood, J. G. (1935). Statistical Mechanics of Fluid Mixtures. *The Journal of Chemical Physics*, Vol.3, No.5, pp. 300-313

Laibinis, P. E.; Nuzzo, R. G. & Whitesides, G. M. (1992). Structure of Monolayers Formed by Coadsorption of Two n-alkanethiols of Different Chain Lengths on Gold and Its Relation to Wetting. *The Journal of Physical Chemistry*, Vol.96, No.12, pp. 5097-5105

Levtsova, O. V.; Antonov, M. Y.; Mordvintsev, D. Y.; Utkin, Y. N.; Shaitan, K. V. & Kirpichnikov, M. P. (2009). Steered Molecular Dynamics Simulations of Cobra Cytotoxin Interaction with Zwitterionic Lipid Bilayer: No Penetration of Loop Tips into Membranes. *Computational Biology and Chemistry*, Vol.33, No.1, pp. 29-32

Li, A. J. & Nussinov, R. (1998). A Set of van der Waals and Coulombic Radii of Protein Atoms for Molecular and Solvent-Accessible Surface Calculation, Packing Evaluation, and Docking. *Proteins*, Vol.32, No.1, pp.111-127

Liphardt, J.; Onoa, B.; Smith, S. B.; Tinoco, I. & Bustamante, C. (2001). Reversible Unfolding of Single RNA Molecules by Mechanical Force. *Science*, Vol.292, No.5517, pp. 733-737

Liphardt, J.; Dumont, S.; Smith, S. B.; Tinoco, I. & Bustamante, C. (2002). Equilibrium Information from Nonequilibrium Measurements in an Rxperimental Test of Jarzynski's Equality. *Science*, Vol.296, No.5574, pp. 1832-1835

Lomize, M. A.; Lomize, A. L.; Pogozheva, I. D. & Mosberg, H. I. (2006). OPM: Orientations of Proteins in Membranes Database. *Bioinformatics*, Vol.22, No.5, pp. 623-625

Love, J. C.; Estroff, L. A.; Kriebel, J. K.; Nuzzo, R. G. & Whitesides, G. M. (2005). Self-Assembled Monolayers of Thiolates on Metals as a Form of Nanotechnology. *Chemical Reviews*, Vol.105, No.4, pp. 1103-1169.

Marrink, S.; Berger, O.; Tieleman, P. & Jahnig, F. (1998). Adhesion Forces of Lipids in a Phospholipid Membrane Studied by Molecular Dynamics Simulations. *Biophysical Journal*, Vol.74, No.2, pp. 931-943

Nordgren, C. E.; Tobias, D. J.; Klein, M. L. & Blasie, J. K. (2002). Molecular Dynamics Simulations of a Hydrated Protein Vectorially Oriented on Polar and Nonpolar Soft Surfaces. *Biophysical Journal*, Vol.83, No.6, pp. 2906-2917

Nose, S. (1984). A Unified Formulation of the Constant Temperature Molecular Dynamics Methods. *The Journal of Chemical Physics*, Vol.81, No.1, pp. 511-519

Ostuni, E.; Grzybowski, B. A.; Mrksich, M.; Roberts, C. S. & Whitesides G. M. (2003). Adsorption of Proteins to Hydrophobic Sites on Mixed Self-Assembled Monolayers. *Langmuir*, Vol.19, No.5, pp. 1861-1872

Park, S. & Schulten, K. (2004). Calculating Potentials of Mean Force from Steered Molecular Dynamics Simulations. *The Journal of Chemical Physics*, Vol.120, No.13, pp. 5946-5961

Park, S.; Khalili-Araghi, F.; Tajkhorshid, E. & Schulten, K. (2003). Free Energy Calculation from Steered Molecular Dynamics Simulations Using Jarzynski's Equality. *The Journal of Chemical Physics*, Vol.119, No.6, pp. 3559-3566

Porter, M. D.; Bright, T. B.; Allara, D. L. & Chidsey, C. E. D. (1987). Spontaneously organized molecular assemblies. 4. Structural characterization of n-alkyl thiol monolayers on gold by optical ellipsometry, infrared spectroscopy, and electrochemistry. *Journal of the American Chemical Society*, Vol.109, No.12, pp. 3559-3568

Prime, K.L. & Whitesides, G.M. (1991). Self-Assembled Organic Monolayers: Model Systems for Studying Adsorption of Proteins at Surfaces. *Science*, Vol.252, No.5009, pp. 1164-1167

Ramstein, J. & Lavery, R. (1988). Energetic Coupling between DNA Bending and Base Pair Opening. *Proceedings of the National Academy of Sciences of the United States of America*, Vol.85, No.19, pp. 7231-7235

Reynolds, J. A., Gilbert, D. B. & Tanford, C. (1974). Empirical Correlation between Hydrophobic Free Energy and Aqueous Cavity Surface Area. *Proceedings of the National Academy of Sciences of the United States of America*, Vol.71, No.8, pp. 2925-2927

Ryckaert, J.-P. & Bellemans, A. (1978). Molecular Dynamics of Liquid Alkanes. *Faraday Discussions of the Chemical Society*, Vol.66, pp. 95-106

Schuler, L. & Gunsteren, W. F. van (2000). On the Choice of Dihedral Angle Potential Energy Functions for n-Alkanes. *Molecular Simulation*, Vol.25, No.5, pp. 301-319

Sivaraman, T.; Kumar, T. K. S.; Chang, D.-K.; Lin, W.-Y. & Yu, C. (1998). Events in the Kinetic Folding Pathway of a Small, All Beta-Sheet Protein. *The Journal of Biological Chemistry*, Vol.273, No.17, pp. 10181-10189

Sivaraman, T.; Kumar, T. K. S.; Hung, K.-W.; & Yu, C. (2000). Comparison of the Structural Stability of Two Homologous Toxins Isolated from the Taiwan Cobra (Naja naja atra) Venom. *Biochemistry*, Vol.39, No.30, pp. 8705-8710

Smith, P. E. & Pettitt, B. M. (1994). Modeling Solvent in Biomolecular Systems. *The Journal of Physical Chemistry*, Vol.98, No.39, pp. 9700-9711

Smith, R. K., Lewis, P. A. & Weiss, P. S. (2004). Patterning Self-Assembled Monolayers. *Progress in Surface Science*, Vol.75, No.1-2, pp. 1-68

Sotomayor, M. & Schulten, K. (2007). Single-Molecule Experiments in Vitro and in Silico. *Science*, Vol.316, No.5828, pp. 1144-1148

Steinbach, P. J. & Brooks, B. R. (1994). New Spherical-Cutoff Methods for Long-Range Forces in Macromolecular Simulation. *Journal of Computational Chemistry*, Vol.15, No.7, pp. 667-683

Sue, S.-C.; Jarrell, H. C.; Brisson, J. R. & Wu. W.-g. (2001). Dynamic Characterization of the Water Binding Loop in the P-Type Cardiotoxin: Implication for the Role of the Bound Water Molecule. *Biochemistry*, Vol.40, No.43, pp. 12782–12794

Tamada, K.; Hara, M. & Sasabe, H. (1997). Surface Phase Behavior of n-alkanethiol Self-Assembled Monolayers Adsorbed on Au (111): An Atomic Force Microscope Study. *Langmuir*, Vol.13, No.6, pp. 1558-1566

Tobias, D. J.; Mar, W.; Blasie, J. K. & Klein, M. L. (1996). Molecular Dynamics Simulations of a Protein on Hydrophobic and Hydrophilic Surfaces. *Biophysical Journal*, Vol.71, No.6, pp. 2933-2941

Torrie, G. M. & Valleau, J. P. (1977). Nonphysical Sampling Distributions in Monte Carlo Free-Energy Estimation: Umbrella Sampling. *Journal of Computational Physics*, Vol.23, No.2, pp. 187-199

Tupper, K. J. & Brenner, D. W. (1994). Compression-Induced Structural Transition in a Self-Assembled Monolayer. *Langmuir*, Vol.10, No.7, pp. 2335-2338

van Gunsteren, W. F. & Berendsen, H. J. C. (1990). Computer Simulation of Molecular Dynamics: Methodology, Applications, and Perspectives in Chemistry. *Angewandte Chemie International Edition in English*, Vol.29, No.9, pp. 992-1023

van der Spoel, D.; Lindahl, E.; Hess, B.; Groenhof, G.; Mark, A. E. & Berendsen, H. J. C. (2005). GROMACS: Fast, Flexible, and Free. *Journal of Computational Chemistry*, Vol.26, No.16, pp. 1701-1718

White, S. & Wimley, W. (1994). Peptides in Lipid Bilayers: Structural and Thermodynamic Basis for Partitioning and Folding. *Current Opinion in Structural Biology*, Vol.4, No.1, pp. 79-86

Ytreberg, F. M.; Swendsen, R. H. & Zuckerman, D. M. (2006). Comparison of Free Energy Methods for Molecular Systems. *The Journal of Chemical Physics*, Vol.125, No.18, pp. 184114

Zheng, J.; Li, L.; Chen, S. & Jiang, S. (2004). Molecular Simulation Study of Water Interactions with Oligo (Ethylene Glycol)-Terminated Alkanethiol Self-Assembled Monolayers. *Langmuir*, Vol.20, No.20, pp. 8931-8938

Zheng, J.; Li, L.; Tsao, H.-K.; Sheng, Y.-J.; Chen, S. & Jiang, S. (2005). Strong Repulsive Forces between Protein and Oligo (Ethylene Glycol) Self-Assembled Monolayers: a Molecular Simulation Study. *Biophysical Journal*, Vol.89, No.1, pp. 158-166

Zhou, J.; Zheng, J. & Jiang, S. (2004). Molecular Simulation Studies of the Orientation and Conformation of Cytochrome c Adsorbed on Self-Assembled Monolayers. *The Journal of Physical Chemistry B*, Vol.108, No.45, pp. 17418-17424

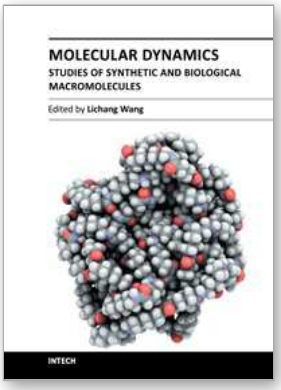

Molecular Dynamics - Studies of Synthetic and Biological Macromolecules

Edited by Prof. Lichang Wang

ISBN 978-953-51-0444-5
Hard cover, 432 pages
Publisher InTech
Published online 11, April, 2012
Published in print edition April, 2012

Molecular Dynamics is a two-volume compendium of the ever-growing applications of molecular dynamics simulations to solve a wider range of scientific and engineering challenges. The contents illustrate the rapid progress on molecular dynamics simulations in many fields of science and technology, such as nanotechnology, energy research, and biology, due to the advances of new dynamics theories and the extraordinary power of today's computers. This second book begins with an introduction of molecular dynamics simulations to macromolecules and then illustrates the computer experiments using molecular dynamics simulations in the studies of synthetic and biological macromolecules, plasmas, and nanomachines. Coverage of this book includes: Complex formation and dynamics of polymers Dynamics of lipid bilayers, peptides, DNA, RNA, and proteins Complex liquids and plasmas Dynamics of molecules on surfaces Nanofluidics and nanomachines

How to reference
In order to correctly reference this scholarly work, feel free to copy and paste the following:

Shih-Wei Hung, Pai-Yi Hsiao and Ching-Chang Chieng (2012). Studies of Cardio Toxin Protein Adsorption on Mixed Self-Assembled Monolayers Using Molecular Dynamics Simulations, Molecular Dynamics - Studies of Synthetic and Biological Macromolecules, Prof. Lichang Wang (Ed.), ISBN: 978-953-51-0444-5, InTech, Available from: http://www.intechopen.com/books/molecular-dynamics-studies-of-synthetic-and-biological-macromolecules/studies-of-ctx-protein-adsorption-on-mixed-sams-surfaces-using-molecular-dynamics-simulations

INTECH
open science | open minds

InTech Europe
University Campus STeP Ri
Slavka Krautzeka 83/A
51000 Rijeka, Croatia
Phone: +385 (51) 770 447
Fax: +385 (51) 686 166
www.intechopen.com

InTech China
Unit 405, Office Block, Hotel Equatorial Shanghai
No.65, Yan An Road (West), Shanghai, 200040, China
中国上海市延安西路65号上海国际贵都大饭店办公楼405单元
Phone: +86-21-62489820
Fax: +86-21-62489821

© 2012 The Author(s). Licensee IntechOpen. This is an open access article distributed under the terms of the Creative Commons Attribution 3.0 License, which permits unrestricted use, distribution, and reproduction in any medium, provided the original work is properly cited.